# PRE-STACK SPLIT-STEP FOURIER DEPTH MIGRATION IN THE $p_O$-$p_S$ DOMAIN

by

M.C. Tanis[1,2], A.W. Mulder[3], P.L. Stoffa[1,2]

M.K. Sen[1], J. Fokkema[3]

**Institute for Geophysics**

**The University of Texas at Austin**

**8701 N. Mopac Blvd.**

**Austin, TX. 78759**

1 Institute for Geophysics, The University of Texas at Austin

2 Department of Geological Sciences, The University of Texas at Austin

3 Delft University of Technology, The Netherlands

**UTIG Technical Report No. 133**

**January, 1995**

## TABLE OF CONTENTS

# Abstract

In this report, post-stack split-step Fourier migration method is extended to migrate pre-stack data. The point of departure is a representation of the pre-stack data in the source and receiver slowness domain. As in the original post-stack split-step migration algorithm, the subsurface is assumed to have only smooth lateral velocity variations. By choosing relative instead of absolute coordinates, the algorithm is made suitable to migrate individual plane wave sections, which are the input data for this algorithm. The decomposition of the data into plane waves is done by slant-stacking.

Constant offset Kirchhoff migration can be used to construct an approximate subsurface image with the advantage of requiring only several constant offset sections from the seismic line. As more constant offset sections are migrated, the image improves if the migration velocity is known. By analogy, plane wave migration can also be performed using a Kirchhoff migration scheme but compared to a Kirchhoff approach, phase-shift plane wave migration has the advantage of being computationally more efficient.

This algorithm also offers some computational advantages over pre-stack shot record migration in that only a limited number of plane wave sections are required to construct a reasonable image of subsurface. The algorithm is tested on 2D synthetic plane wave sections and the results are compared with the output of a Kirchhoff plane wave migration algorithm.

# Introduction



Originally, split-step Fourier depth migration was applied to post-stack seismic data by Stoffa et al., 1990. In the split-step migration algorithm, the earth is assumed to be horizontally layered with small lateral velocity changes within each layer. To migrate the data over one layer, two phase-shifts are applied. The first is based on the average slowness function in the depth interval and is applied in the frequency-wavenumber domain. This is identical to Gazdag's (1978) phase-shift migration. The second phase-shift is based on the lateral velocity perturbation (Stoffa et al., 1990), and is applied in the frequency-space domain to correct for lateral velocity differences in the layer.

Generally, pre-stack seismic data can be migrated in many different ways. These depend on the way the data are organized e.g., shot records, constant offset sections etc. and the method employed e.g., Kirchhoff , finite-difference, phase-shift etc.

The split-step Fourier algorithm can easily be extended to migrate shot gathers. This *shot record migration* is a natural extension of post-stack split-step Fourier migration as outlined in Stoffa et al. (1990), where each shot record is migrated separately by downward continuing shot and receiver wave fields independently and correlating them at each depth level to construct an image. Alternatively, the imaging condition can be changed so that the direct wave travel times can be used to replace the extrapolation of the source wave field and applied as a phase term (Tanis, 1993).

*Full migration*, on the other hand, migrates the total wavefield, recorded by a range of receivers, at the same time. Source and receiver records are propagated downward together for each layer and an image is directly constructed at every level. This migration requires sorting of the data constantly between common source and common receiver gathers to apply the phase-shifts on both the source and receiver gathers successively. Flowcharts outlining these schemes are displayed in Figures 1 and 2.

Both of these methods can be quite time consuming especially when applied to a large data set, such as those required in modern marine 3D surveys. In shot record migration, each shot record needs to be migrated separately and the final image is obtained by adding all the individually migrated sections. So, this approach requires many independent migrations to construct an image of subsurface.

For the full migration scheme the solution is even worse because the data need to be sorted back and forth at each depth level between common shot gathers and common receiver gathers. This causes the algorithm to be very slow and hard to implement efficiently because of the large memory requirements for any reasonable survey.

# Method

In this report, an alternative pre-stack split-step Fourier migration method is presented. The solution to this algorithm is obtained in the po-ps domain, where the wavefield is decomposed into plane waves. In the $p_o$-$p_s$ domain, the wavefield is no longer represented by its wave numbers but by its horizontal slowness, $p_o$ and $p_s$, where $p_o$ is related to the angle with which a plane wave arrives at the receiver position and $p_s$ is related to the difference between the angle of the plane waves at the source and the angle at the receiver.

Developing the migration scheme in the $p_o$-$p_s$ domain offers some computational advantages over the above mentioned shot-record and full migration algorithms. One advantage is that by using the double square root (DSR) (Claerbout, 1984) in the $p_o$-$p_s$ domain both the source and receiver wavefield are downward continued simultaneously. Another advantage is that similar to a constant offset Kirchhoff migration in this domain the image can be approximated by only migrating a small number of constant $p_o$ sections.

To be able to evaluate a single plane wave section, the offset ray parameter, $p_o$, is split into two parts: the starting part, $p_o$ and a perturbation part, $\Delta p_o$. Initially the plane wave is constant and is related to the value of the plane wave angle at the receiver. The varying part is the difference between the initial part and the true $p_o$. Since the velocity is assumed to be smoothly varying in the model, this varying part should also be small.

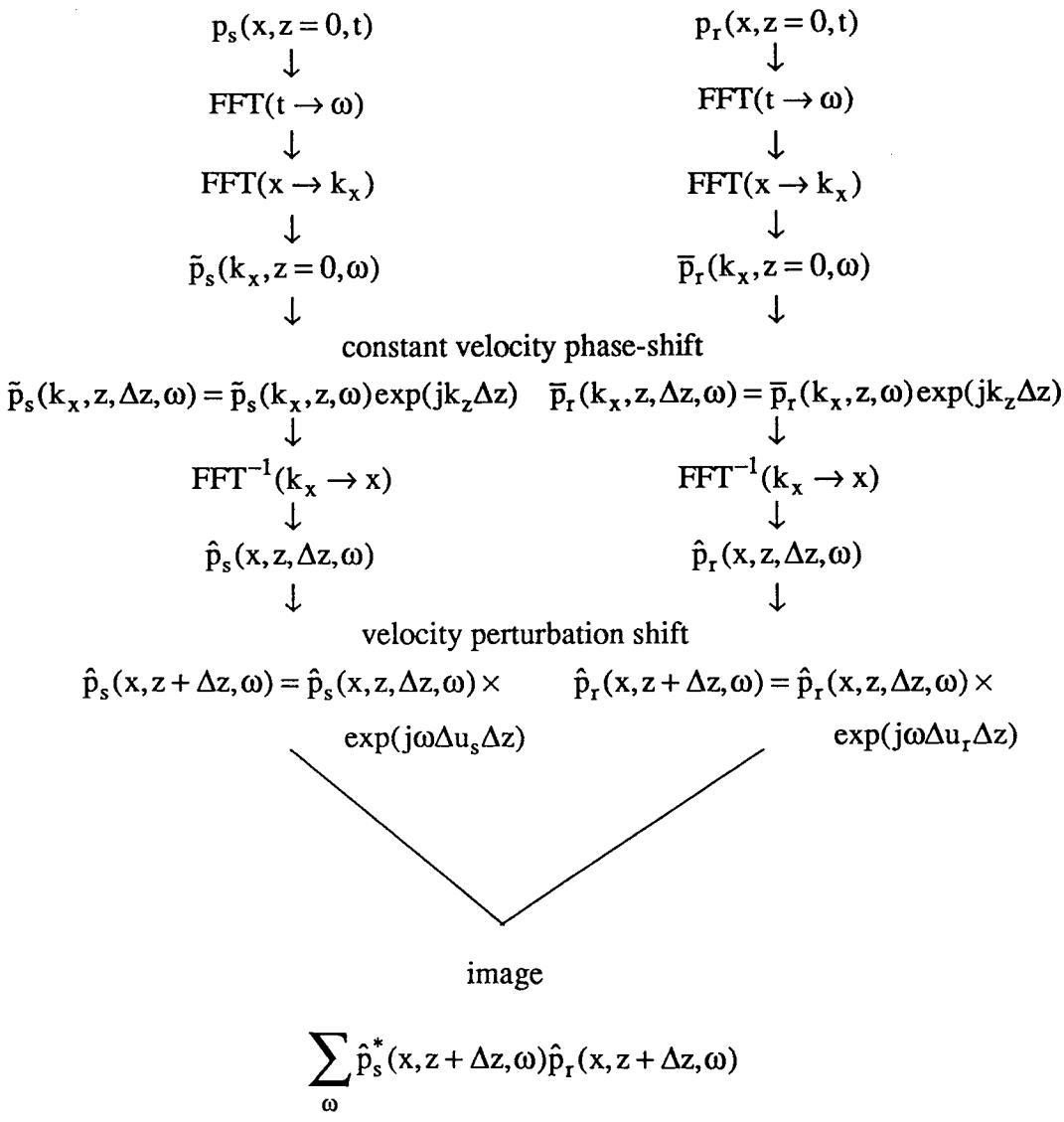


***Figure 1. Shot record migration scheme.***

$$p(x_r, z | x_s, z, t)$$

$$\downarrow$$

$$\mathrm{FFT}(t \rightarrow \omega)$$

$$\downarrow$$

$$\mathrm{FFT}(x_r \rightarrow p_r, x_s \rightarrow p'_s)$$

$$\downarrow$$

$$\tilde{\tilde{p}}(p_r, z = 0 | p'_s, z = 0, \omega)$$

$$\downarrow$$

apply the phase-shift for the receiver coordinate

$$\tilde{\tilde{p}}(p_r, z, \Delta z | p'_s, z = 0, \omega) = \tilde{\tilde{p}}(p_r, z | p'_s, z = 0, \omega) \exp(j\omega \Gamma^r \Delta z)$$

$$\downarrow$$

resort to common receiver gathers

$$\downarrow$$

$$\tilde{\tilde{p}}(p_r, z, \Delta z | p'_s, z, \Delta z, \omega) = \tilde{\tilde{p}}(p_r, z, \Delta z | p'_s, z, \omega) \exp(j\omega \Gamma^{s'} \Delta z)$$

$$\downarrow$$

$$\mathrm{FFT}^{-1}(p_r \rightarrow x_r, p'_s \rightarrow x_s)$$

$$\downarrow$$

$$\hat{p}(x_r, z, \Delta z | x_s, z, \Delta z, \omega)$$

$$\downarrow$$

apply second phase-shift

$$\hat{p}(x_r, z + \Delta z | x_s, z, \Delta z, \omega) = \hat{p}(x_r, z, \Delta z | x_s, z, \Delta z, \omega) \exp(j\omega \Delta u_s \Delta z)$$

$$\downarrow$$

resort to common source gathers

$$\downarrow$$

$$\hat{p}(x_r, z + \Delta z | x_s, z + \Delta z, \omega) = \hat{p}(x_r, z + \Delta z | x_s, z, \Delta z, \omega) \exp(j\omega \Delta u_r \Delta z)$$

$$\downarrow$$

get the image

$$\sum_{\omega} \hat{p}(x_r, z + \Delta z | x_s, z + \Delta z, \omega)$$

***Figure 2. Full migration scheme.***

# Theory



The full migration scheme will be the starting point to obtain the migration equation in the $p_o$-$p_s$ domain. In this scheme, the total wavefield at each depth level is given by the following equation in the Laplace-domain:

$$\hat{p}(x_r, z+\Delta z | x_s, z+\Delta z, s) =$$

$$\exp(s\Delta u_z(x_r)\Delta z + s\Delta u_z(x_s)\Delta z) \times$$

$$F_s^{-1} F_r^{-1}\left\{\exp(s\Gamma^r \Delta z + s\Gamma^{s'}\Delta z) F_s F_r(\hat{p}(x_r, z | x_s, z, s))\right\}, \qquad (1)$$

where $\hat{p}(x_r, z|x_s, z, s)$ is the total wavefield at depth level z, $x_r$ is the receiver position, $x_s$ is the source position, $\Delta u_z(x_s)$ and $\Delta u_z(x_r)$ are the slowness perturbation terms, $\Gamma^{s'}$ and $\Gamma^r$ are the vertical wave numbers for the source and receiver coordinates and defined as.

$$\Gamma^{s'} = (u^2 - (\alpha_s')^2)^{\frac{1}{2}} \text{ and } \Gamma^r = (u^2 - (\alpha_r)^2)^{\frac{1}{2}},$$

$F_S$, $F_S{}^{-1}$ and $F_r$, $F_r{}^{-1}$ represent forward and inverse Fourier transforms between spatial domain and the wave number domain and defined for the forward transforms as

$$\tilde{p}(x_r, z | js\alpha_s', z, s) = \frac{1}{2\pi}\int_{x_s} dx_s \exp(js\alpha_s' x_s)\hat{p}(x_r, z | x_s, z, s),$$

$$\tilde{p}(js\alpha_r, z | x_s, z, s) = \frac{1}{2\pi}\int_{x_r} dx_r \exp(js\alpha_r x_r)\hat{p}(x_r, z | x_s, z, s),$$

and for the inverse transforms as

$$\hat{p}(x_r, z | x_s, z, s) = \frac{1}{2\pi}\int_{s\alpha_s'} ds\alpha_s' \exp(-js\alpha_s' x_s)\tilde{p}(x_r, z | js\alpha_s', z, s),$$

$$\hat{p}(x_r, z | x_s, z, s) = \frac{1}{2\pi}\int_{s\alpha_r} ds\alpha_r \exp(-js\alpha_r x_r)\tilde{p}(js\alpha_r, z | x_s, z, s).$$

To be able to use this equation in practice, the following variables are chosen:

$$s = j\omega, \qquad p_r = j\alpha_r, \qquad p'_s = j\alpha'_s,$$

where $p'_s$ is the angle which the ray coming from the source makes with the vertical and $p_r$ is the angle made by the vertical at the receiver position. These two, $p'_s$ and $p_r$, will respectively be called the true source angle and the receiver angle (Figure 3).

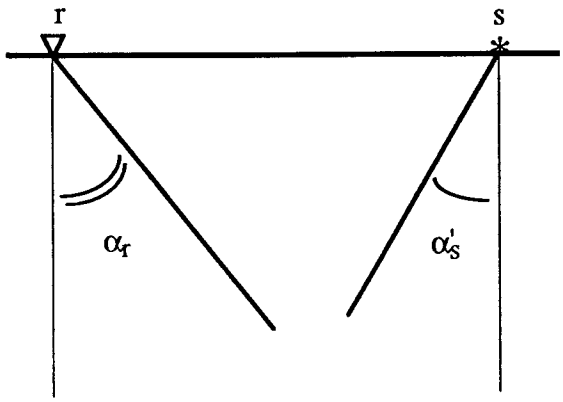


***Figure 3. Absolute coordinates.***

Upon rewriting, we get:

$$\hat{p}(x_r, z+\Delta z | x_s, z+\Delta z, \omega) =$$

$$\exp(j\omega\Delta u_z(x_r)\Delta z + j\omega\Delta u_z(x_s)\Delta z) \times$$

$$\int_{p_r} dp_r \exp(-j\omega p_r x_r) \int_{p'_s} dp'_s \exp(-j\omega p'_s x_s)(\exp(j\omega\Gamma^r\Delta z + j\omega\Gamma^{s'}\Delta z) \times$$

$$\int_{x_r} dx_r \exp(j\omega p_r x_r) \int_{x_s} dx_s \exp(j\omega p'_s x_s)\hat{p}(x_r, z | x_s, z, \omega)). \qquad (2)$$

As mentioned earlier, migration with this algorithm is time consuming. To try to improve the computational efficiency, the following coordinate transformation is chosen;

$$x_o = x_s - x_r, \qquad p_o = p_r, \qquad p_s = p_r + p'_s,$$

where $x_o$ is the offset or the distance between the source and the receiver position. The corresponding slowness, $p_r$, $p_s$, $p_s'$ and $p_o$ correspond to the sine of the respective angles traveled by the velocity. The offset angle, $\alpha_o$, is equal to the receiver angle, $\alpha_r$, and $\alpha_s$, the new source angle is the sum of the receiver angle and the true source angle. Since the receiver angle $\alpha_r$ and the true source angle $\alpha'_s$ have, in most cases, opposite signs, the new source angle, $\alpha_s$ is the true angle $\alpha'_s$ reduced by the angle $\alpha_r$. The definition of these angles is presented in Figure 4.

As long as the distance between source and receiver position is large compared to the measuring depth, the angle $\alpha_s$ will be smaller than the true source angle. The deeper the reflector, the more $\alpha_s$ is reduced.

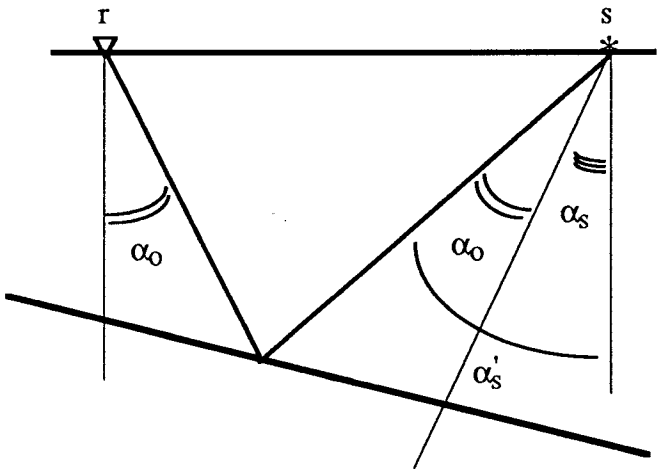


***Figure 4. Relative coordinates.***

With these new quantities, the vertical slownesses become

$$\Gamma^o = (u^2 - p_o^2)^{\frac{1}{2}}, \qquad \Gamma^s = (u^2 - (p_s - p_o)^2)^{\frac{1}{2}}.$$

Now without any additional approximation the migration algorithm will have the following form:

$$\hat{p}(x_o + x_s, z + \Delta z | x_s, z + \Delta z, \omega) =$$

$$\exp(j\omega\Delta u_z(x_o + x_s)\Delta z + j\omega\Delta u_z(x_s)\Delta z) \times$$

$$\int_{p_o} dp_o \exp(-j\omega p_o x_o) \int_{p_s} dp_s \exp(-j\omega p_s x_s)(\exp(j\omega\Gamma^o\Delta z + j\omega\Gamma^s\Delta z) \times$$

$$\int_{x_o} dx_o \exp(j\omega p_o x_o) \int_{x_s} dx_s \exp(j\omega p_s x_s)\hat{p}(x_o + x_s, z | x_s, z, \omega)), \qquad (3)$$

If slant-stacking is applied to the input data by using the following definition;

$$\hat{p}(p_o, x_s, z | x_s, z, \omega) = \int_{x_o} dx_o \exp(j\omega p_o x_o)\hat{p}(x_o + x_s, z | x_s, z, \omega),$$

then Equation (3) can be rewritten as

$$\hat{p}(p_o, x_s, z + \Delta z | x_s, z + \Delta z, \omega) =$$

$$\exp(j\omega\Delta u_z(p_o, x_s)\Delta z + j\omega\Delta u_z(x_s)\Delta z) \times$$

$$\int_{p_s} dp_s \exp(-j\omega p_s x_s)(\exp(j\omega\Gamma^o\Delta z + j\omega\Gamma^s\Delta z) \times$$

$$\int_{x_s} dx_s \exp(j\omega p_s x_s)\hat{p}(p_o, x_s, z | x_s, z, \omega)). \qquad (4)$$

The above representation make it possible to migrate individual constant $p_o$-sections separately. Although $p_o$ starts out as a constant (because after slant-stacking we have gathered one $p_o$ for all shot records), after the plane wave is propagated backward and encounters a lateraly varying velocity field, the initial $p_o$ will be changed. However, to accommodate a spatially varying $p_o$, the offset ray parameter, $p_o(x,z)$ is defined as the sum of the initial $p_o$ and a spatially varying perturbation term, $\Delta p_o(x,z)$, i.e.,

$$p_o(x,z) = \bar{p}_o + \Delta p_o(x,z),$$

where $\bar{p}_o$ is the initial $p_o$ value at the receiver location and $\Delta p_o(x,z)$ is the horizontal slowness perturbation caused by velocity variations at the dipping interfaces. This perturbation term $\Delta p_o(x,z)$ is assumed to be small, which is consistent with the basic assumption that the velocity was assumed to be slowly-varying laterally. How this $p_o$-perturbation influences the vertical wave numbers $\Gamma^o$ and $\Gamma^s$ is shown in the appendix.

Now using the above definition and the new phase-shift term obtained in the appendix, the downward continuation equation can be rewritten as

$$\begin{aligned}
&\hat{p}(p_o, x_s, z+\Delta z | x_s, z+\Delta z, \omega) = \\
&\quad \exp(j\omega \Delta u_z(p_o, x_s)\Delta z + j\omega \Delta u_z(x_s)\Delta z) \times \\
&\quad \int_{p_s} dp_s \exp(-j\omega p_s x_s)(\exp(j\omega \bar{\Gamma}^o \Delta z + j\omega \bar{\Gamma}^s \Delta z) \times \\
&\quad \exp(-j\omega \bar{\Gamma}^s \Delta z \frac{2\alpha(\bar{p}_o \Delta p_o - p_s \Delta p_o)}{u^2 - (p_s - \bar{p}_o)^2 - 2\beta(\bar{p}_o \Delta p_o - p_s \Delta p_o)}) \times \\
&\quad \exp(-j\omega \bar{\Gamma}^o \Delta z \frac{2\alpha \bar{p}_o \Delta p_o}{u^2 - \bar{p}_o^2 - 2\beta \bar{p}_o \Delta p_o}) \times \\
&\quad \int_{x_s} dx_s \exp(j\omega p_s x_s) \hat{p}(p_o, x_s, z | x_s, z, \omega)).
\end{aligned} \tag{5}$$

Since it is expected that $p_s$ will be small in a slowly varying medium, especially when the target is deep in the subsurface, it can be neglected in the second phase-shift term. Consequently, the final equation reduces to the following form;

$$\hat{p}(p_o, x_s, z+\Delta z | x_s, z+\Delta z, \omega) =$$

$$\exp(j\omega\Delta u_z(p_o, x_s)\Delta z + j\omega\Delta u_z(x_s)\Delta z) \times$$

$$\exp(-2j\omega\overline{\Gamma}^o\Delta z \frac{2\alpha\overline{p}_o\Delta p_o}{u^2 - \overline{p}_o^2 - 2\beta\overline{p}_o\Delta p_o}) \times$$

$$\int_{p_s} dp_s \exp(-j\omega p_s x_s)(\exp(j\omega\overline{\Gamma}^o\Delta z + j\omega\overline{\Gamma}^s\Delta z) \times$$

$$\int_{x_s} dx_s \exp(j\omega p_s x_s)\hat{p}(p_o, x_s, z | x_s, z, \omega)). \qquad (6)$$

A flowchart of this algorithm is displayed in Figure 5.

$$\hat{p}(p_o, x_s, z | x_s, z, t)$$

$$\downarrow$$

$$\text{FFT}(t \rightarrow \omega)$$

$$\downarrow$$

$$\text{FFT}(x_s \rightarrow p_s)$$

$$\downarrow$$

$$\hat{p}(p_o, x_s, z = 0 | p_s, z = 0, \omega)$$

$$\downarrow$$

apply the phase-shifts for the constant velocity part

$$\hat{p}(p_o, x_s, z, \Delta z | p_s, z, \Delta z, \omega) = \hat{p}(p_o, x_s, z | p_s, z, \omega) \exp(j\omega \bar{\Gamma}^o \Delta z + j\omega \bar{\Gamma}^s \Delta z)$$

$$\downarrow$$

$$\text{FFT}^{-1}(p_s \rightarrow x_s)$$

$$\downarrow$$

$$\hat{p}(p_o, x_s, z, \Delta z | x_s, z, \Delta z, \omega)$$

$$\downarrow$$

apply second phase-shift

$$\hat{p}(p_o, x_s, z + \Delta z | x_s, z + \Delta z, \omega) = \hat{p}(p_o, x_s, z, \Delta z | x_s, z, \Delta z, \omega) \times$$

$$\exp(j\omega \Delta u_z(p_o, x_s) \Delta z + j\omega \Delta u_z(x_s) \Delta z) \times$$

$$\exp\left(-2j\omega \bar{\Gamma}^o \Delta z \frac{2\alpha \bar{p}_o \Delta p_o}{u^2 - \bar{p}_o^2 - 2\beta \bar{p}_o \Delta p_o}\right)$$

$$\downarrow$$

get the image

$$\sum_{\omega} \hat{p}(p_o, x_s, z + \Delta z | x_s, z + \Delta z, \omega)$$

***Figure 5. po-ps domain migration scheme.***

## Synthetic Examples

The algorithm outlined in Figure 5 was used to migrate synthetic plane wave sections. In addition, the same plane wave sections were migrated using a plane wave Kirchhoff migration scheme (Akbar et al., 1994) for comparison. Figure 6 shows the velocity model, which was used to compute the synthetic plane wave seismic sections. The dip of the second layer is 20 degrees and the velocity contrast at the dipping interface is about 35%, changing from 1.7 km/sec above to 2.3 km/sec below. A total of five plane wave sections were used in this migration example. These are -0.2 sec/km, -0.1 sec/km, 0. sec/km, 0.1 sec/km and 0.2 sec/km.

The migration parameters used for all of the migrated sections are as follows; trace spacing $\Delta x$=10 m, depth sample $\Delta z$=10 m, input time sample $\Delta t$=4 msec, number of shots 200, number of depth samples 250 and the number of time samples 1000.

The output migrated sections obtained from both algorithms are very similar. Migrated section for $p_o$'s 0.0, -0.1 and -0.2 sec/km (Figure 7, 8 and 9) are nearly identical except for amplitude diferences since an amplitude correction was applied to the Kirchhoff plane wave migrated sections. The plane wave migrated sections for $p_o$ = 0.1 and 0.2 sec/km (Figure 10 and 11), however, show slight depth differences for the third reflector. The split-step Fourier method seems to have shifted that particular layer in depth by a few samples.

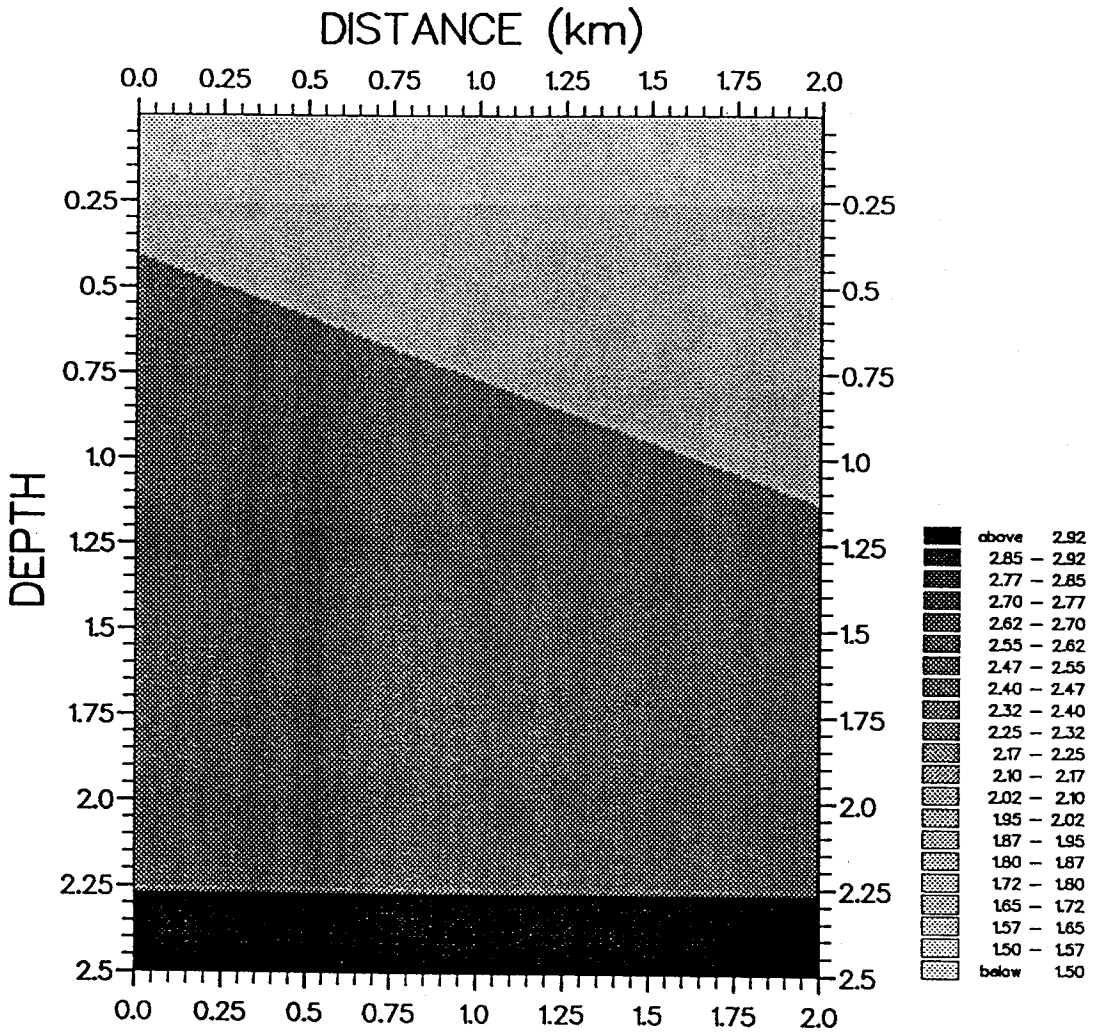


Figure 6. Velocity model used for migration.

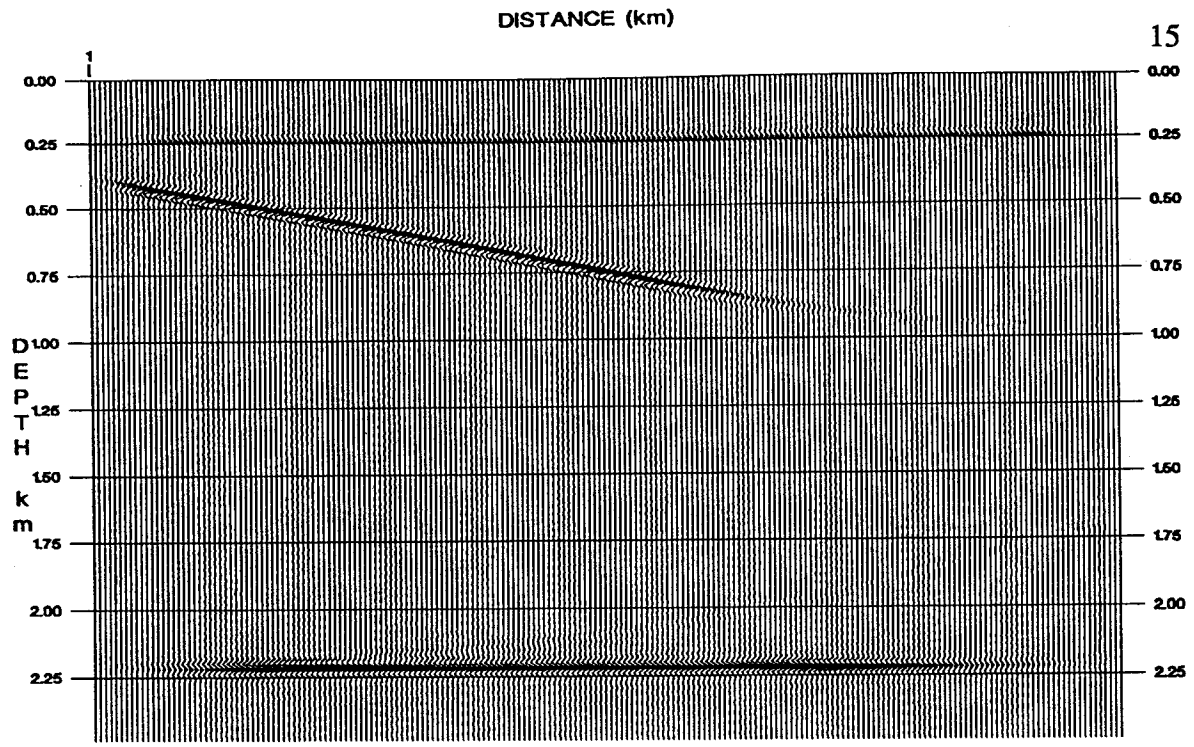


(a)

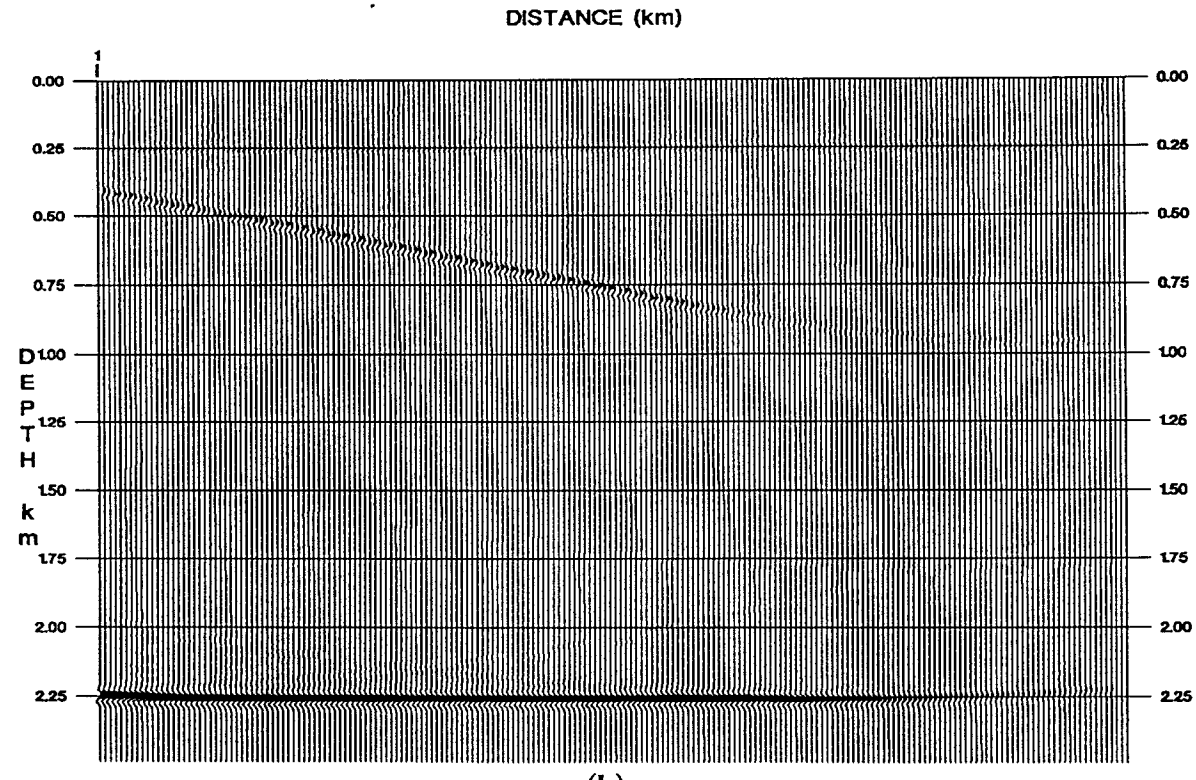


(b)

**Figure 7.** Migrated constant plane wave sections for $p_o$= 0.0 sec/km (a) by split-step Fourier migration method, and (b) by plane wave Kirchhoff migration.

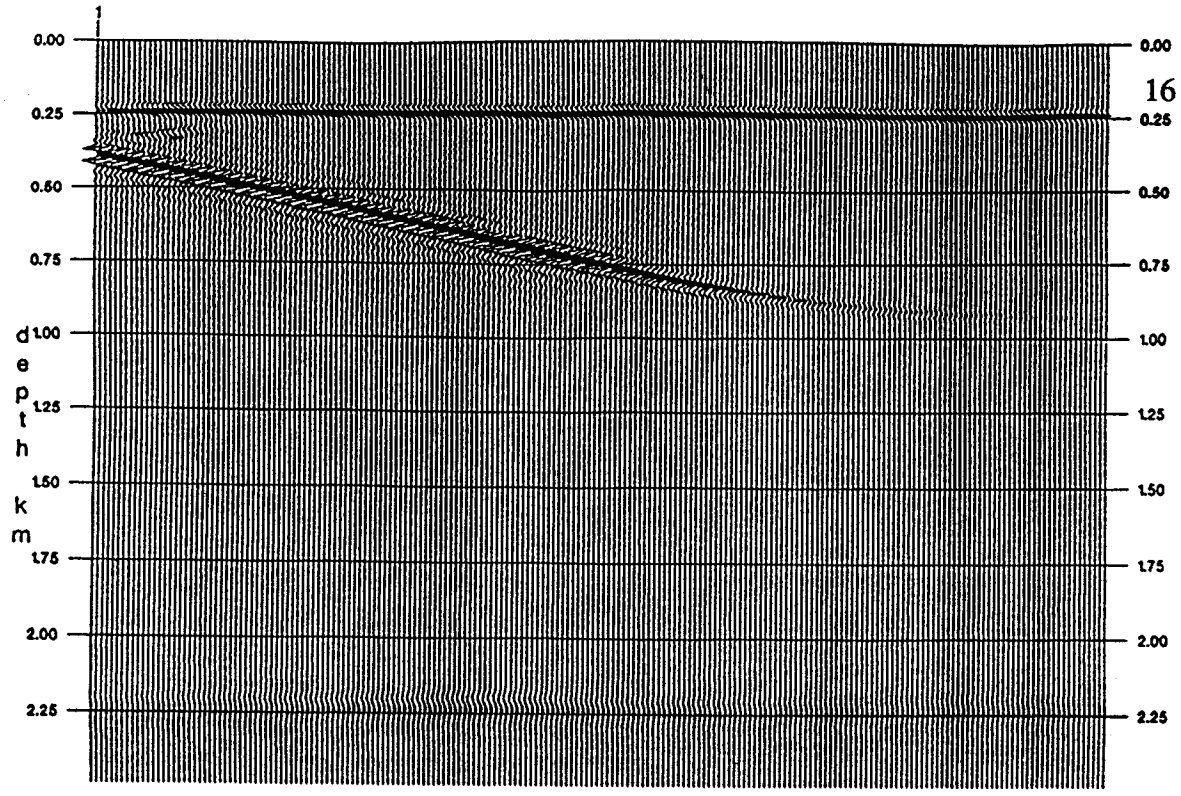


(a)

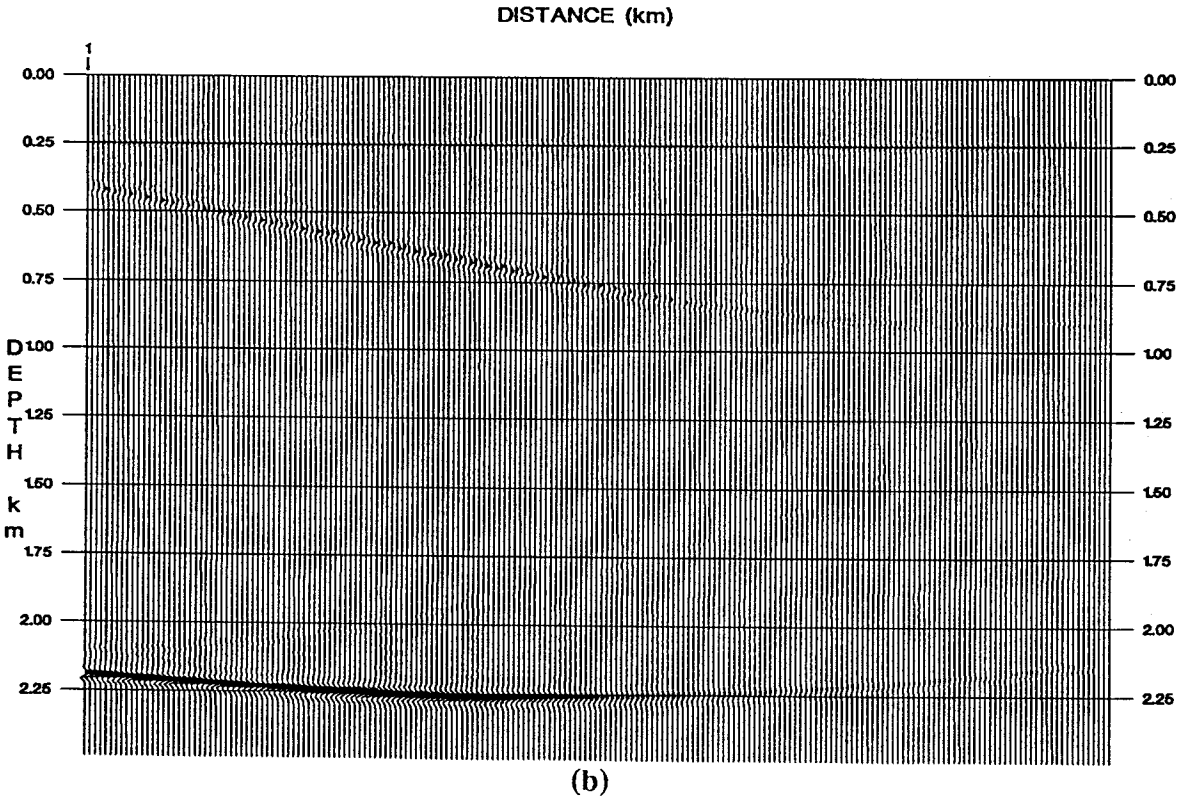


(b)

**Figure 8.** Migrated constant plane wave sections for $p_o$= -0.1sec/km (a) by split-step Fourier migration method, and (b) by plane wave Kirchhoff migration.

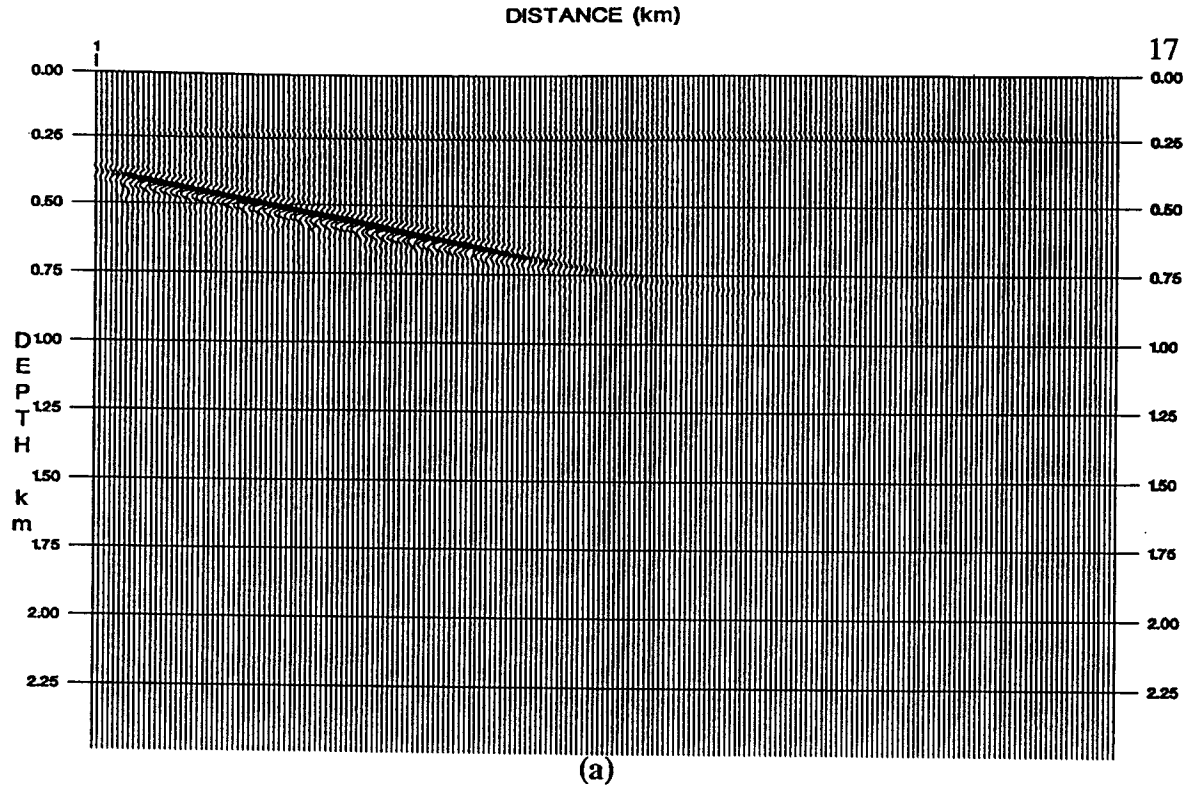


(a)

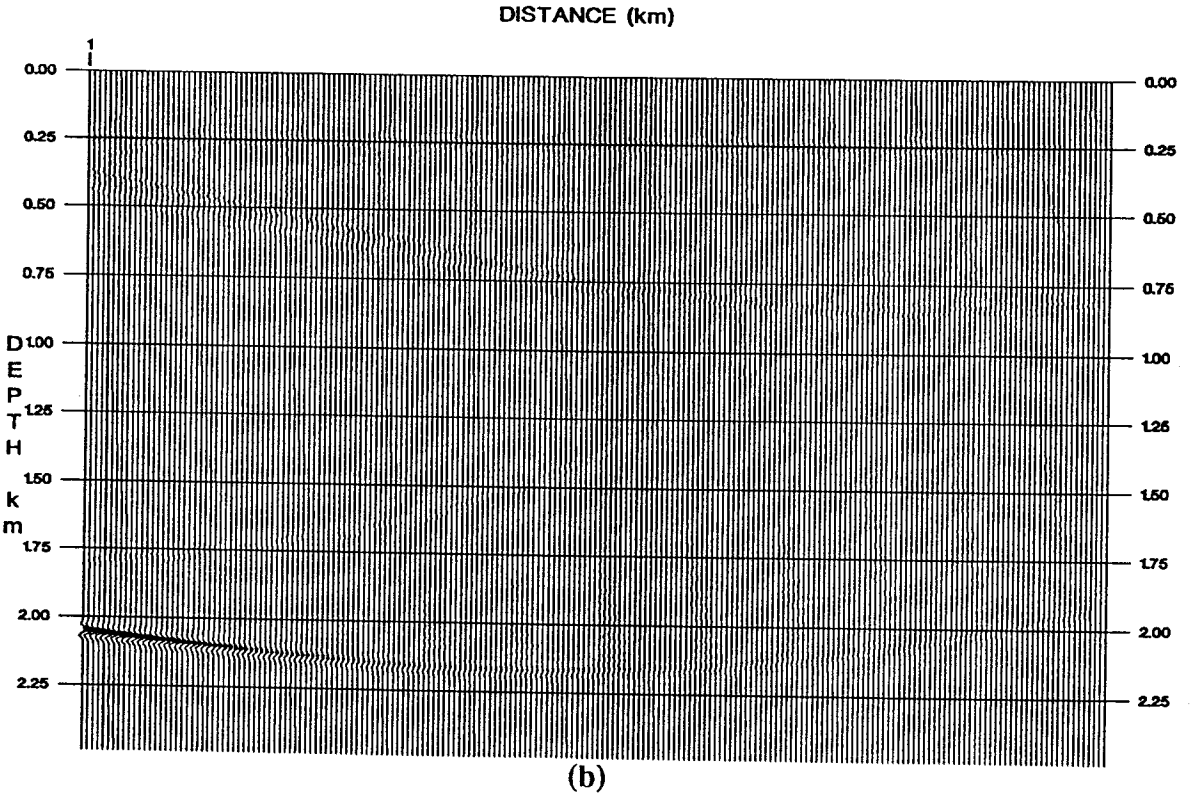


(b)

**Figure 9.** Migrated constant plane wave sections for $p_o$= -0.2 sec/km (a) by split-step Fourier migration method, and (b) by plane wave Kirchhoff migration.

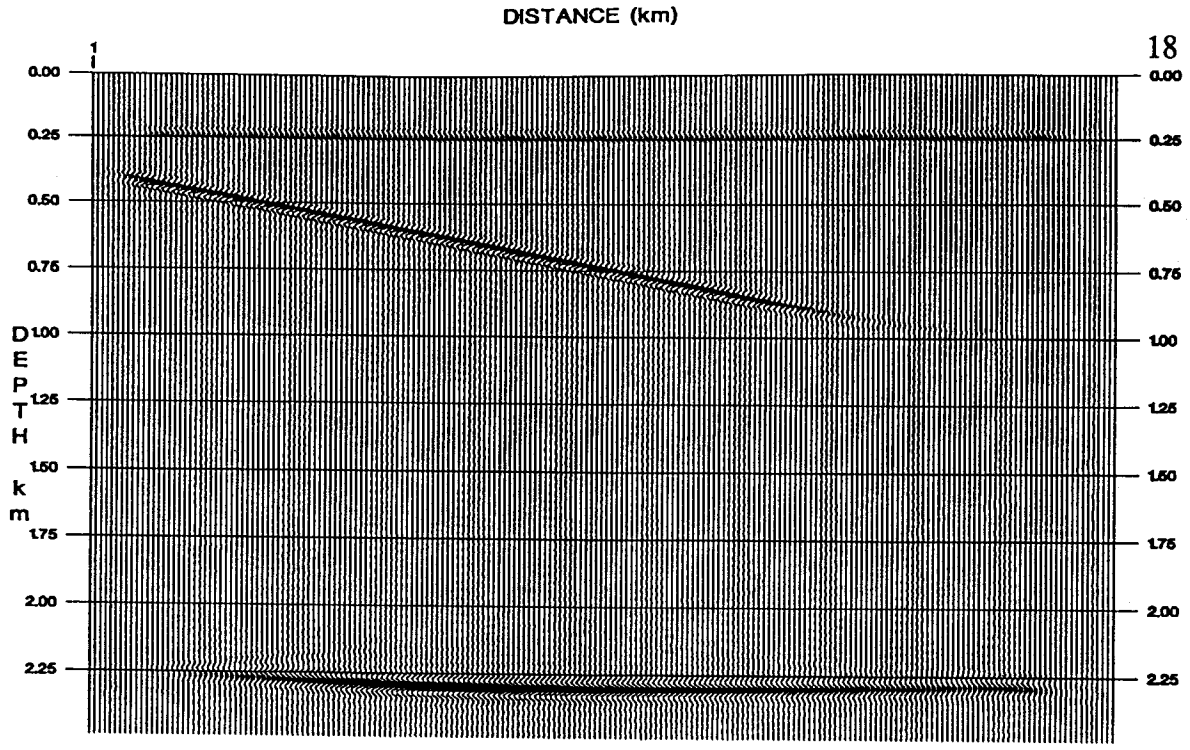


(a)

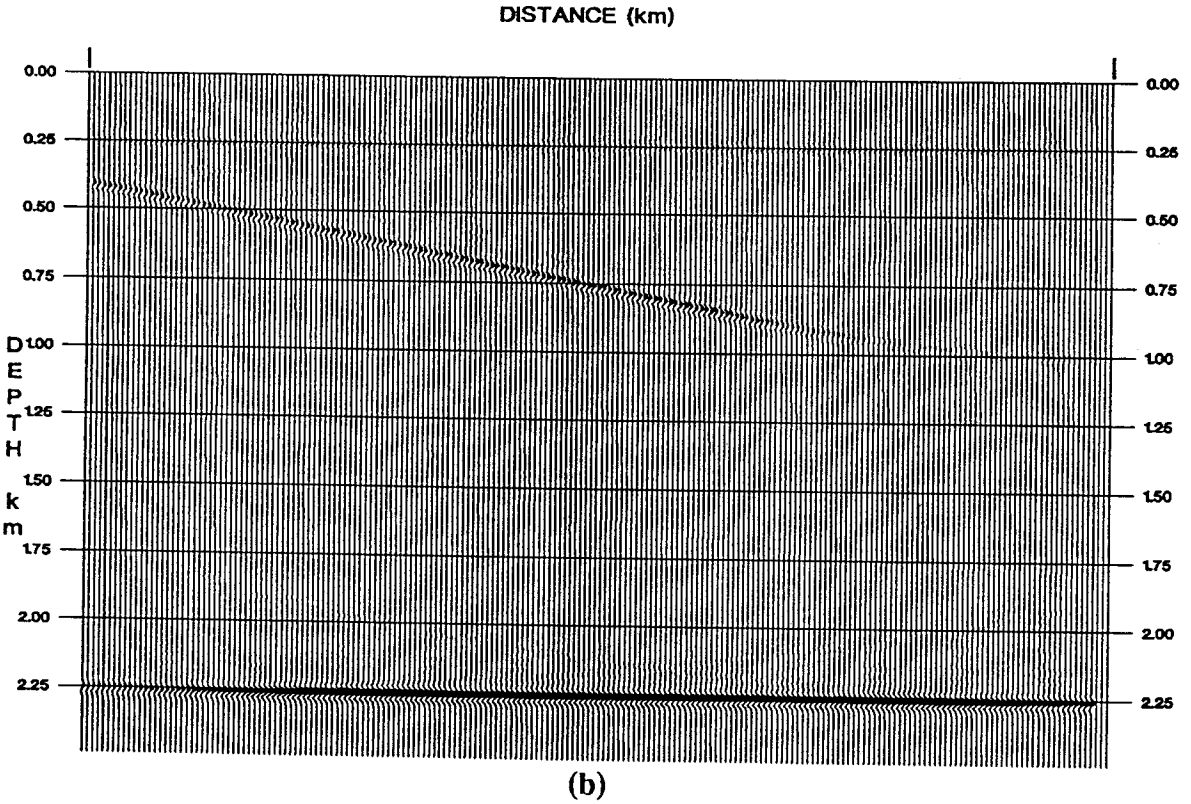


(b)

**Figure 10.** Migrated constant plane wave sections for $p_o$= +0.1sec/km (a) by split-step Fourier migration method, and (b) by plane wave Kirchhoff migration.

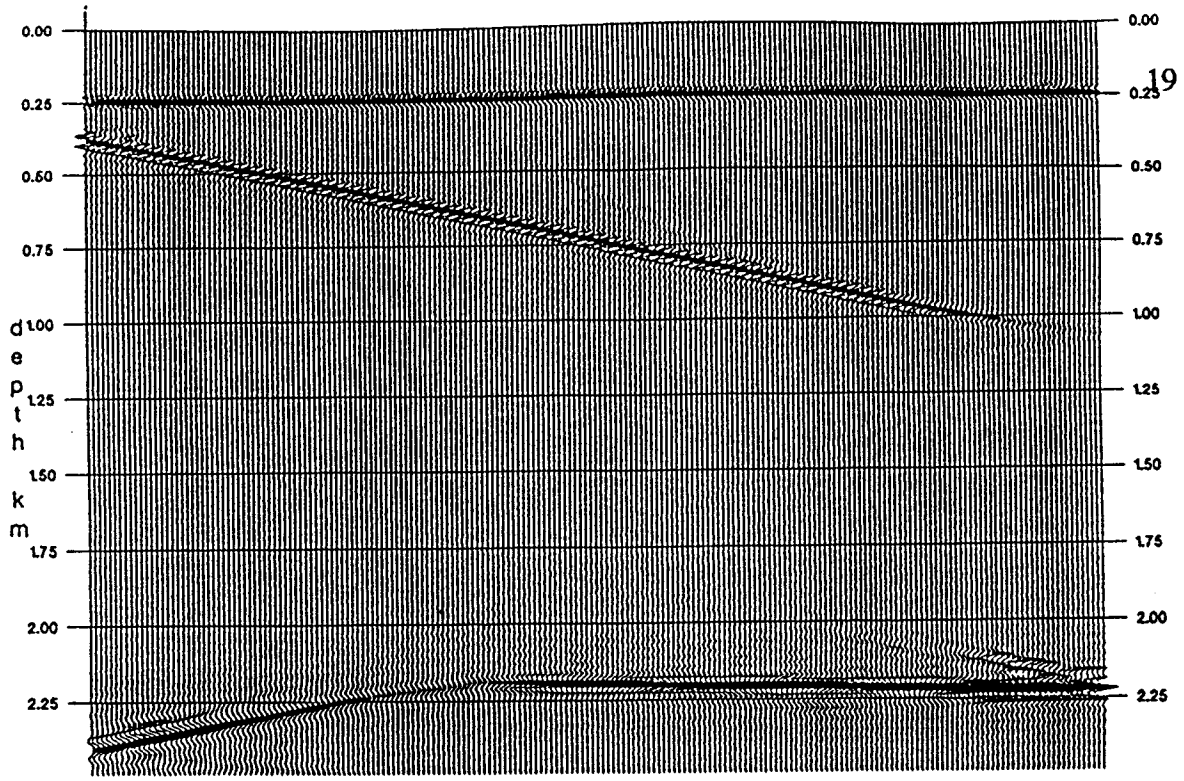


(a)

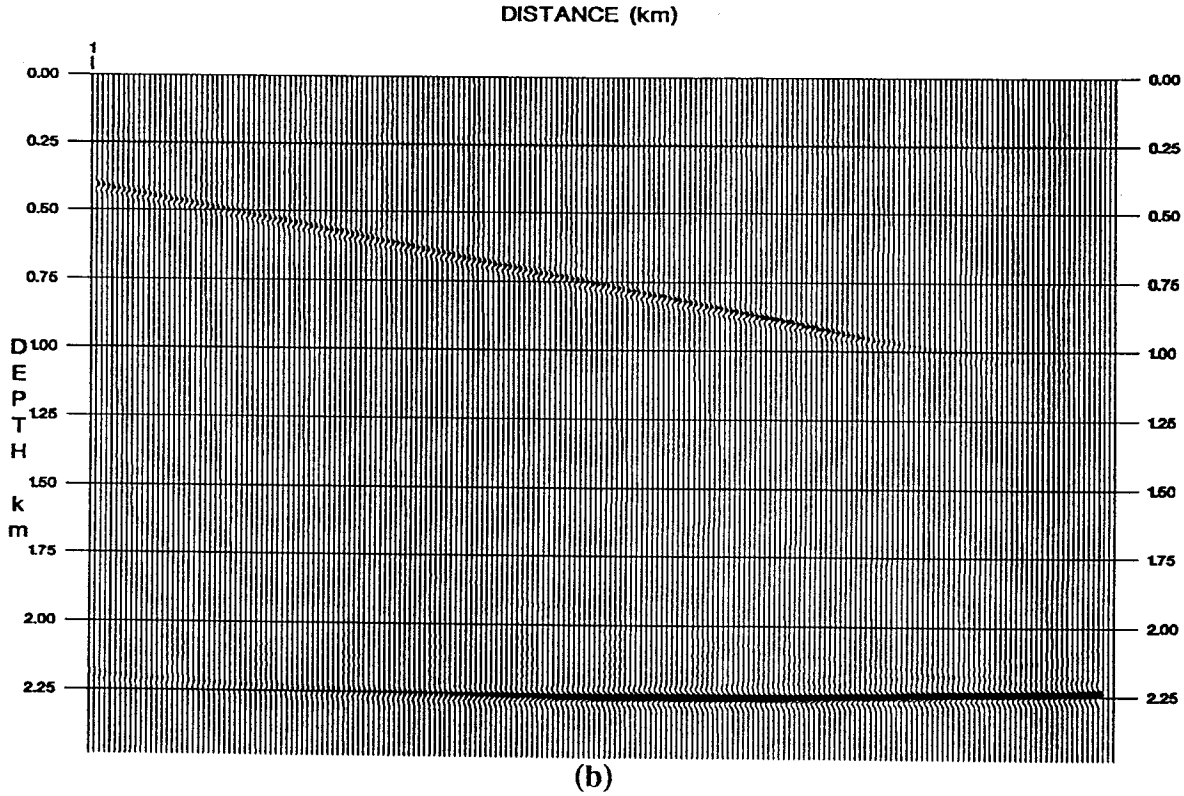


(b)

**Figure 11.** Migrated constant plane wave sections for $p_o$= +0.2 sec/km (a) by split-step Fourier migration method, and (b) by plane wave Kirchhoff migration.

# Conclusions

In this report, split-step Fourier migration method has been extended and applied to pre-stack data. The starting point for this algorithm was the pre-stack migration representation in the source-receiver angular slowness domain. The solution was obtained in the $p_o$-$p_s$ domain for computational efficiency. Two assumptions were employed in the solution; the lateral velocity variations in the subsurface are assumed to be small and the difference between the source angle and the receiver angle in the perturbation term is small; therefore, it can be neglected.

The algorithm is applied to migrate 2D synthetic plane wave seismic sections and the results are compared with the results obtained from plane wave Kirchhoff migration method. The results suggest that the pre-stack split-step Fourier algorithm is efficient and reasonably accurate. However, more accurate result can be obtained by relaxing some of the assumptions employed at the cost of higher computational time. The method should be useful in cases of modest geologic structures where the assumptions are not violated. In these cases, pre-stack depth migration can be performed very efficiently.

# Appendix

The vertical slownesses in the phase-shift term are

$$\Gamma^s = (u^2 - (p_s - p_o)^2)^{\frac{1}{2}},$$

and

$$\Gamma^o = (u^2 - p_o^2)^{\frac{1}{2}}.$$

Using $p_o = \bar{p}_o + \Delta p_o$ the vertical slowness for the source will become

$$\Gamma^s = (u^2 - (p_s^2 - 2p_s(\bar{p}_o + \Delta p_o) + (\bar{p}_o + \Delta p_o)^2)^{\frac{1}{2}})$$

$$= (u^2 - (p_s - \bar{p}_o)^2)^{\frac{1}{2}}(1 - \frac{2\bar{p}_o\Delta p_o + 2p_s\Delta p_o}{u^2 - (p_s - \bar{p}_o)^2})^{\frac{1}{2}}.$$

By definition $\left(1 - X^2\right)^{\frac{1}{2}} \approx \frac{\alpha X^2}{1 - \beta X^2}$. Applying it to the above vertical slowness, we get

$$\Gamma^s \approx (u^2 - (p_s - \bar{p}_o)^2)^{\frac{1}{2}}(1 - \frac{2\alpha(\bar{p}_o\Delta p_o + p_s\Delta p_o)}{u^2 - (p_s - \bar{p}_o)^2 - 2\beta(\bar{p}_o\Delta p_o + p_s\Delta p_o)}),$$

where $\alpha = \frac{1}{2}$ and $\beta = \frac{1}{4}$.

The same approximation can be used on the offset vertical slowness term which then becomes,

$$\Gamma^o \approx (u^2 - \bar{p}_o^2)^{\frac{1}{2}}(1 - \frac{2\alpha\bar{p}_o\Delta p_o}{u^2 - \bar{p}_o{}^2 - 2\beta\bar{p}_o\Delta p_o}).$$

New vertical slowness terms are now presented as

$$\Gamma^s \approx \overline{\Gamma}^s\left(1-\frac{2\alpha(\overline{p}_o\Delta p_o + p_s\Delta p_o)}{u^2-(p_s-\overline{p}_o)^2-2\beta(\overline{p}_o\Delta p_o + p_s\Delta p_o)}\right),$$

$$\Gamma^o \approx \overline{\Gamma}^o\left(1-\frac{2\alpha\overline{p}_o\Delta p_o}{u^2-\overline{p}_o{}^2-2\beta\overline{p}_o\Delta p_o}\right),$$

where

$$\overline{\Gamma}^s = (u^2-(p_s-\overline{p}_o)^2)^{\frac{1}{2}},$$

$$\overline{\Gamma}^o = (u^2-\overline{p}_o^2)^{\frac{1}{2}}.$$

# References

Akbar, F.E., Sen, M.K., Stoffa, P.L., 1994, Pre-stack plane-wave Kirchhoff depth migration using a cluster of workstations: SEG expanded abstracts, p.225-228.

Claerbout, J.F., 1985, *Imaging the Earth's Interior:* Blackwell Science Publishers, Oxford, England.

Mulder, A.W., 1994, Pre-stack split-step Fourier migration, Master's thesis, Delft University of Technology, The Netherlands.

Stoffa, P.L., Fokkema, J.T, Freire, R.M.L., and Kessinger, W.P., 1990, Split-step Fourier migration: Geophysics, v. 55, p.410-421.

Tanis, M.C., 1993, A comparison of migration methods in laterally varying media, Master's thesis, The University of Texas at Austin, Austin, TX.